Independent Estimation of Input and Measurement Delays for a Hybrid Vertical Spring–Mass–Damper via Harmonic Transfer Functions

İsmail Uyanık*, M. Mert Ankaralı, Noah J. Cowan****
Uluç Saranlı*, Ömer Morgül* and Hitay Özbay***

**Department of Electrical and Electronics Engineering, Bilkent University, 06800 Ankara, Turkey (e-mail: {uyanik,morgul,hitay}@ee.bilkent.edu.tr).*
***Department of Mechanical Engineering, Johns Hopkins University, Baltimore, MD 21218, USA (e-mail: {mertankarali,ncowan}@jhu.edu)*
****Department of Computer Engineering, Middle East Technical University, 06800 Ankara, Turkey (e-mail: saranli@ceng.metu.edu.tr)*

Abstract:
System identification of rhythmic locomotor systems is challenging due to the time-varying nature of their dynamics. Even though important aspects of these systems can be captured via explicit mechanics-based models, it is unclear how accurate such models can be while still being analytically tractable. An alternative approach for rhythmic locomotor systems is the use of data-driven system identification in the frequency domain via harmonic transfer functions (HTFs). To this end, the input–output dynamics of a locomotor behavior can be linearized around a stable limit cycle, yielding a linear, time-periodic system. However, few if any model-based or data-driven identification methods for time-periodic systems address the problem of input and measurement delays in the system. In this paper, we focus on data-driven system identification for a simple mechanical system and analyze its dynamics in the presence of input and measurement delays using HTFs. By exploiting the way input delays are modulated by the periodic dynamics, our results enable the separate, independent estimation of input and measurement delays, which would be indistinguishable were the system linear and time invariant.

Keywords: Time-delay estimation, time-periodic systems, system identification, harmonic transfer functions, legged locomotion.

1. INTRODUCTION

Despite the widespread use of legs by animals to achieve terrestrial locomotion (Full and Tu, 1991; Holmes et al., 2006), the majority of mobile robots use wheels or tracks to move themselves. Unfortunately, this choice impairs mobility and performance on broken and unstable terrain (LaBarbera, 1983), shifting attention to the use of legs in mobile and field robotics (Raibert, 1986), despite significant challenges in the design, modeling, and control of legged robot platforms (Wooden et al., 2010).

Modeling and analysis of even seemingly simple legged systems can be surprisingly complex due to the hybrid dynamics arising from intermittent foot contact as well as challenging nonlinearities in the equations of motion (Ankarali and Saranli, 2010; Saranli et al., 2010; Uyanik et al., 2015c; Westervelt et al., 2007; Grizzle et al., 2001). In this context, modeling of legged behaviors generally rely on a white-box approach, involving careful characterization of individual components in the system and the intended behavior together with informed (but possibly incorrect) "decisions" about what to neglect.

An alternative to such explicit modeling efforts is the use of data-driven system identification techniques. For example, in our previous work (Uyanik et al., 2015a), we proposed a data-driven parametric system identification method for a class of locomotion models exhibiting asymptotically stable limit cycles (Seipel and Holmes, 2007; Altendorfer et al., 2004), with possible applications to similarly structured robotic systems (Saranli et al., 2001; Galloway et al., 2010). Our approach was to approximate system dynamics around the limit-cycle as a linear time-periodic (LTP) system, enabling us to address the input–output system identification problem in the frequency domain using harmonic transfer functions. Since the initial, infinite dimensional LTP approximation was not suitable for a parametric representation, we introduced additional approximations to reduce the model to a finite dimensional piecewise LTI system (maintaining its LTP nature), thereby limiting the

⋆ This material is based on work supported by the National Science Foundation Grants 0845749 and 1230493 (to N. J. Cowan). The authors thank ASELSAN Inc. and TUBITAK for İsmail Uyanık's financial support.
⋆⋆İ. Uyanık and M. M. Ankaralı contributed equally to this work.

parametric degrees of freedom while enabling a practical parametric identification framework.

Such a finite dimensional, piecewise LTI representation cannot, however, capture time delays (input, measurement, or internal/transmission), which constitute an inevitable aspect of both biological and artificial locomotor systems with significant impact on behavior. For instance, sensor latency and delays can significantly limit neural control performance (Cowan et al., 2006; Sponberg and Full, 2008; Cowan et al., 2014). In the context of robotics, delays can be introduced by different sources, including communication during teleoperation (Anderson and Spong, 1989), or between multi-agent systems (Tian and Liu, 2008), and latency arising from the computational complexity and filtering associated with processing sensory information such as visual and LiDAR data (Miller III, 1989). Even though these phenomena can often be approximated as pure delays in the system (Kataria et al., 2002), their impact on the stability and performance of the closed loop system can be rather significant and should be carefully taken into account in all stages of the analysis including system identification and the design of controllers.

In this paper, our main contribution is the extension of our prior work on the identification and analysis of robotic legged locomotion (Uyanik et al., 2015a) to explicitly consider input and measurement delays, leaving the modeling of internal system delays as future work. There is a long history of modeling and analyzing delays in both biological (Elzinga et al., 2012; Sponberg and Full, 2008) and robotic (Anderson and Spong, 1989; Kataria et al., 2002) control systems. Most of this previous work, however, uses linear time-invariant (LTI) models to approximate system dynamics and their nominal trajectories. As we have shown in our previous work, such LTI representations can be inadequate in capturing time-varying characteristics of locomotor behaviors where nominal trajectories are large limit-cycles with distinct hybrid phases (Uyanik et al., 2015a; Kiemel et al., 2013; Ankarali and Cowan, 2014; Uyanik et al., 2015b). We now show that linear analysis can still be applied in this context, using the LTP framework to relax the time-invariance assumption, allowing us to identify and analyze input and measurement delays in rhythmic legged locomotor behaviors.

2. BACKGROUND

Our previous work focused on representing the dynamics of clock–driven hybrid legged locomotion models around their limit–cycles as linear time-periodic (LTP) systems. As described in Uyanik et al. (2015a), under some assumptions, the hybrid dynamics of such systems can be approximated with a time-periodic, piecewise LTI system. This formulation constitutes the basis of our analysis and identification framework for the clock-driven legged locomotion models described below.

2.1 Frequency Response of Linear Time Periodic Systems

Many finite-dimensional LTP systems can be described by a state space model of the form

$$\begin{aligned} \dot{x}(t) &= A(t)x(t) + B(t)u(t) \\ y(t) &= C(t)x(t) + D(t)u(t), \end{aligned} \tag{1}$$

where $A(t)$, $B(t)$, $C(t)$, and $D(t)$ are all periodic with period T. Expanding all system matrices, state and output vectors by an infinite Fourier series with pumping frequency $\omega_p = 2\pi/T$ and applying the principle of harmonic balance as explained in Wereley (1991), one can obtain the infinite-dimensional harmonic state space representation of the LTP system as

$$\begin{aligned} s\mathcal{X} &= (\mathcal{A} - \mathcal{N})\mathcal{X} + \mathcal{B}\mathcal{U} \\ \mathcal{Y} &= \mathcal{C}\mathcal{X} + \mathcal{D}\mathcal{U}, \end{aligned} \tag{2}$$

where the new system parameters are doubly infinite Toeplitz matrices representing the harmonics of the state, output and control signals. The doubly infinite input matrix, which modulates the input frequency to different harmonic frequencies, is defined as $\mathcal{N} :=$ blockdiag$\{jn\omega_p I\}, \forall n \in Z$.

Now the harmonic transfer function, G, can be defined as

$$G := \mathcal{C}[sI - (\mathcal{A} - \mathcal{N})]^{-1}\mathcal{B} + \mathcal{D}\ , \tag{3}$$

assuming that $(sI - (\mathcal{A} - \mathcal{N}))$ is invertible. Subsequently, the input–output relationship of the LTP system can be written as

$$Y(j\omega) = \sum_{m=-\infty}^{\infty} G_m(j\omega)U(j\omega - jm\omega_p). \tag{4}$$

Details and proofs on the derivation of the harmonics transfer functions can be found in Wereley (1991).

2.2 Data-Driven System Identification with Harmonic Transfer Functions

Our data-driven identification of harmonic transfer functions begins by truncating the number of harmonics in (4) to $2M + 1$ components. The identification problem is now reduced to the estimation of a finite number of harmonic transfer functions by using available input–output data such as carefully designed chirp signals (Siddiqi, 2001).

Once input–output pairs are obtained, an optimization problem is constructed such that the error between actual and predicted system response is minimized with an additional constraint to enforce smoothness on the estimated transfer functions. Then, the harmonic transfer functions can be found as

$$\hat{\mathbf{G}} = (\mathbf{U^T U} + \alpha(\mathbf{D^2})^{\mathbf{T}}\mathbf{D^2})^{-1}\mathbf{U^T Y}\ , \tag{5}$$

where $\mathbf{D^2}$ is an appropriately defined matrix implementing a second difference operator and α is a manually tuned constant weight for penalizing curvature.

(Note that here, $\mathbf{U}, \mathbf{Y}, \mathbf{G}$ are book-kept slightly differently than U, Y, G, defined above; see Siddiqi (2001) for details.)

3. PIECEWISE LTI DYNAMICS WITH INPUT AND MEASUREMENT DELAYS

3.1 System Model with Input and Measurement Delays

Even though there are many different forms in which delay can be observed in practical systems, our model for input and measurement delays in this paper takes the form of constant, frequency independent time shifts τ_u and τ_y in the action of the input $u(t)$ and the observation of the system output $y(t)$, respectively. If we define two intermediate variables $\bar{u}(t)$ and $\bar{y}(t)$, where

$$\bar{u}(t) = u(t - \tau_u)$$
$$y(t) = \bar{y}(t - \tau_y) \ ,$$

and write the system dynamics using these new variables, we get

$$\dot{x}(t) = \begin{cases} A_0 x(t) + B_0 \bar{u}(t), & \text{if } \mathrm{mod}(t,T) \in [0, \hat{t}) \\ A_1 x(t) + B_1 \bar{u}(t), & \text{if } \mathrm{mod}(t,T) \in [\hat{t}, T) \end{cases}$$
$$\bar{y}(t) = \begin{cases} C_0 x(t) + D_0 \bar{u}(t), & \text{if } \mathrm{mod}(t,T) \in [0, \hat{t}) \\ C_1 x(t) + D_1 \bar{u}(t), & \text{if } \mathrm{mod}(t,T) \in [\hat{t}, T) \end{cases} \quad (6)$$

We intentionally represent in a form that reveals the input–output dynamics between $\bar{u}(t)$ and $\bar{y}(t)$, since the same structure is valid for $u(t)$ and $y(t)$.

The most important benefit of this representation arises from the difficulty of trying to explicitly model delay in the harmonic transfer function framework, which would have required substantial modifications to its derivation as well as the associated system identification method. We will instead adopt a two stage approach. First we will perform system identification on input-output pairs using only the magnitude plots of the non-parametric HTFs and assume that neither the input, nor the output signals are delayed. Then, we will analyze the resulting model in the frequency domain using the phase plots of the non-parametric HTFs to estimate the delays.

3.2 The Effects of Delays on Harmonic Transfer Functions

Since the delayed LTP dynamics of (6) have the same structure with delayless dynamics, the associated input–output relation between $\bar{u}(t)$ and $\bar{y}(t)$ has the same form as (4) in the frequency domain. However, we need the relationship between $u(t)$ and $y(t)$, which are the actual input and output signals of the system. Fortunately, our assumption of fixed time linear delays allows us to express actual input and output signals as a function of their undelayed counterparts in (6) in the frequency domain, satisfying $\bar{U}(w) = U(w)e^{-j\omega\tau_u}$ and $Y(w) = \bar{Y}(w)e^{-j\omega\tau_y}$. Substitution into (4) yields

$$Y(j\omega) = \sum_{m=-\infty}^{\infty} G_m(j\omega) e^{-j[(\omega - m\omega_p)\tau_u + \omega\tau_y]} U(j(\omega - m\omega_p)) \quad (7)$$

where the terms

$$H_m(j\omega) := G_m(j\omega) e^{-j[(\omega - m\omega_p)\tau_u + \omega\tau_y]}$$

correspond to the harmonic transfer functions between the actual input $U(w)$, and the actual measurement $Y(w)$ for the delayed system. Comparing the HTFs for the zero-delay input–output representation, $G_m(j\omega)$, with their delayed counterparts, $H_m(j\omega)$, we will show that we can separately identify input and measurement delays in the system. This will be the main contribution of this paper.

We begin by noting that the harmonic transfer functions both with and without delay have the same magnitudes. This is easily shown through the definition of $H_m(j\omega)$, with

$$\begin{aligned} |H_m(j\omega)| &= |G_m(j\omega) e^{-j[(\omega - m\omega_p)\tau_u + \omega\tau_y]}|, \\ &= |G_m(j\omega)|. \end{aligned} \quad (8)$$

On the other hand, phase responses with and without delays can be different. More specifically, we have

$$\angle H_m(j\omega) = \angle G_m(j\omega) - [(\omega - m\omega_p)\tau_u + \omega\tau_y] \ . \quad (9)$$

Note that for $m = 0$, these derivations are analogous to LTI systems, where input and measurement delays cannot be distinguished since the fundamental harmonic is phase-shifted according to their sum. More importantly, however, when additional harmonics with $m \neq 0$ are considered, the frequency dependence of contributions from input and measurement delays to the HTF phase shift will be different. This property of harmonic transfer functions allows us to independently estimate the input and measurement delays in an LTP system, which are otherwise indistinguishable for LTI systems.

We incorporate both of these observations in our approach to estimate system delays. We begin by using input–output pairs $u(t)$ and $y(t)$ from the original, delayed system to obtain the harmonic transfer functions $H_m(j\omega)$. Since the magnitudes of these HTF components are identical to their counterparts for the undelayed version of the system, we can use our previously proposed method to estimate unknown parameters for an explicitly constructed, undelayed system model based on $|H_m(j\omega)|$ alone (Uyanik et al., 2015a). This parametric model gives us the phase responses of the undelayed system, $\angle G_m(j\omega)$, as a reference against which the phase characteristics of the delayed system, $\angle H_m(j\omega)$ can be compared. This comparison allows independent and robust computation of the input and measurement delays, τ_u and τ_y, when multiple harmonics $m \in \mathbb{Z}$ are considered to as closely satisfy (9) as possible.

4. APPLICATION: A HYBRID, VERTICAL, SPRING–MASS SYSTEM

4.1 System Dynamics

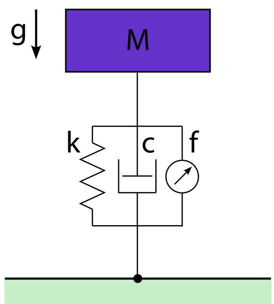

Fig. 1. Hybrid Vertical Spring–Mass–Damper Model.

In this section, we illustrate the application of our method to estimate input and measurement delays for a hybrid vertical spring–mass–damper system that incorporates some of the fundamental aspects of legged locomotion while admitting a model in the form of (6). Fig. 1 illustrates the model, which consists of a point mass attached to a massless leg with a linear spring, k, a viscous damping, c, as well as a force transducer f.

Classical legged locomotion models often incorporate *stance* and *flight* phases distinguished by different contact states of their toe with the ground. We preserve this hybrid structure, but differentiate these two phases by only changing the damping coefficient in the leg across the two phases ($c = 0$ during flight and $c > 0$ during stance) and keeping the toe affixed to the ground at all times rather than altogether eliminating the interaction of the

Table 1. Estimation results for input and measurement delay via different harmonic transfer functions.

Exp.	*Actual Delays*		G_0 *Estimates*		G_{-1} *Estimates*				G_1 *Estimates*			
	τ_u [ms]	τ_y [ms]	$\hat{\tau}_{u+y}$ [ms]	PE_{u+y}	$\hat{\tau}_u$ [ms]	PE_u	$\hat{\tau}_y$ [ms]	PE_y	$\hat{\tau}_u$ [ms]	PE_u	$\hat{\tau}_y$ [ms]	PE_y
#1	0	0	0	-	0	-	1.6	-	0	-	0	-
#2	0	50	49.9	0.20 %	0	-	51.6	3.2 %	0	-	47.5	5.0 %
#3	0	100	99.9	0.10 %	0	-	101.6	1.6 %	0	-	97.5	2.5 %
#4	40	0	40.0	0 %	41.1	2.75 %	0	-	38	5.0 %	0	-
#5	40	50	90.1	0.10 %	41.7	4.25 %	49.7	0.6 %	41.2	3.0 %	47.6	4.8 %
#6	40	100	140.1	0.07 %	41.9	4.75 %	99.5	0.5 %	41.2	3.0 %	95.1	4.9 %
#7	80	0	80.1	0.12 %	81.7	2.12 %	0.5	-	76.7	4.1 %	2.9	-
#8	80	50	130.1	0.08 %	81.8	2.25 %	50.4	0.8 %	76.8	4.0 %	52.4	4.8 %
#9	80	100	180.1	0.55 %	82.1	2.62 %	100.2	0.2 %	76.9	3.9 %	102.7	2.7 %

leg with the ground during flight. This simplified structure allows us to express the system in the form of (6) and derive closed-form expressions for the harmonic transfer functions associated with this system, while preserving essential features of locomotor behaviors such as the presence of distinct hybrid phases with different continuous dynamics.

The force transducer in the leg is used for two purposes. Since there is damping in the system, its first function is to compensate for energy losses, enforcing a stable limit cycle. It is also used as an exogenous input to the system around its limit cycle, effectively implementing $u(t)$ in (6) to support the system identification process. More formally, the linear actuator force is chosen as $f(t) = f_0(t) + u(t)$, where $f_0(t)$ term implements a periodic input to maintain limit cycle and $u(t)$ is used to introduce small periodic perturbations for system identification.

The equations of motion for the hybrid vertical spring–mass–damper model are hence given by

$$m\ddot{x} = \begin{cases} -mg - c\dot{x} - k(x - x_0) + f(t), & \text{if } \dot{x} > 0 \\ -mg - k(x - x_0) + f(t), & \text{otherwise.} \end{cases} \quad (10)$$

Simulation studies in subsequent sections use the following parameters for this model; $g = 9.81$, $k = 200$, $c = 2$, $m = 1$ and $x_0 = 0.2$. All simulations are implemented in Matlab environment by using standard ordinary differential equation solvers and built-in matrix operations with 1 KHz sampling frequency.

4.2 Theoretical Derivation of Harmonic Transfer Functions for System Dynamics Without Delays

As we noted above, our method for estimating time delays in the system requires fitting a parametric model to the magnitude characteristics of the HTF representation obtained from input–output data. To this end, this section derives parametric, closed-form expressions for HTF components of our example locomotion model of Section 4.1.

We begin by assuming that $f_0(t)$ is appropriately chosen to induce an asymptotically stable limit cycle $\bar{x}(t)$. Changing into "error" coordinates, defined as the deviation from the limit cycle as $\xi := x(t) - \bar{x}(t)$, induces local equations of motion around the limit cycle with

$$\ddot{\xi} = \begin{cases} -c\dot{\xi} - k\xi, & \text{if } \dot{\xi} + \dot{\bar{x}}(t) > 0 \\ -k\xi, & \text{otherwise} \end{cases} \quad (11)$$

Using a switching function $s(\dot{\xi}, t)$, constructed such that $s = 1$, when $\dot{\xi} + \dot{\bar{x}}(t) > 0$ and $s = 0$ otherwise, these dynamics correspond to a piecewise LTI system in the form

$$\begin{bmatrix} \dot{\xi}_1 \\ \dot{\xi}_2 \end{bmatrix} = \begin{bmatrix} 0 & 1 \\ -k & -cs(\dot{\xi}, t) \end{bmatrix} \begin{bmatrix} \xi_1 \\ \xi_2 \end{bmatrix} + \begin{bmatrix} 0 \\ 1 \end{bmatrix} u(t). \quad (12)$$

The only remaining problem is the dependence of the switching function $s(\dot{\xi}, t)$ on the system state. In our previous work, we showed that since $s(\dot{\xi}, t)$ is time-periodic in steady-state, it can be approximated around the limit cycle to only depend on time with $s(\dot{\xi}, t) \approx s(t)$ (Uyanik et al., 2015a). This assumption yields an LTP system, whose state space representation takes the form

$$\begin{bmatrix} \dot{\xi}_1 \\ \dot{\xi}_2 \end{bmatrix} = \begin{bmatrix} 0 & 1 \\ -k & -cs(t) \end{bmatrix} \begin{bmatrix} \xi_1 \\ \xi_2 \end{bmatrix} + \begin{bmatrix} 0 \\ 1 \end{bmatrix} u(t), \quad (13)$$
$$y = [1 \ \ 0] \begin{bmatrix} \xi_1 \\ \xi_2 \end{bmatrix} .$$

Fourier series expansion of $s(t)$, followed by the use of the HTF framework described in Section 2.1, the harmonic transfer functions of our example system can be obtained.

4.3 Identification of Harmonic Transfer Functions from Input–Output Data

We begin by estimating harmonic transfer functions of the linearized dynamics of (13) by using input–output data under input and measurement delay, without assuming any prior knowledge of the state space model. We use $f_0(t) = \cos(2\pi t)$ and $u(t) = 0$ to achieve an asymptotically stable limit cycle and record steady state data.

Subsequently, we start perturbing the limit cycle with an input signal, constructed as the concatenation of nine consecutive, $30s$ long chirp signals.

Each chirp signal is designed to linearly increase in the range $(0, 7]$ Hz over its duration, taking the form

$$u_i(t) = 0.004 \sin(7\pi t^2/30). \quad (14)$$

In contrast, the starting phases of consecutive copies of the chirp signal are chosen to be evenly separated throughout system's period, $T = 1s$ as explained in Section 2.2.

In order to evaluate the performance of our identification method, we present 9 separate experiments with different combinations input and measurement delays, listed in Table 1. We feed the sequence of chirp signals described above with an input delay, τ_u and simulate the system with the input $\bar{u}(t) = u(t - \tau_u)$. We then impose an output delay with $y(t) = \bar{y}(t - \tau_y)$ to simulate the effect

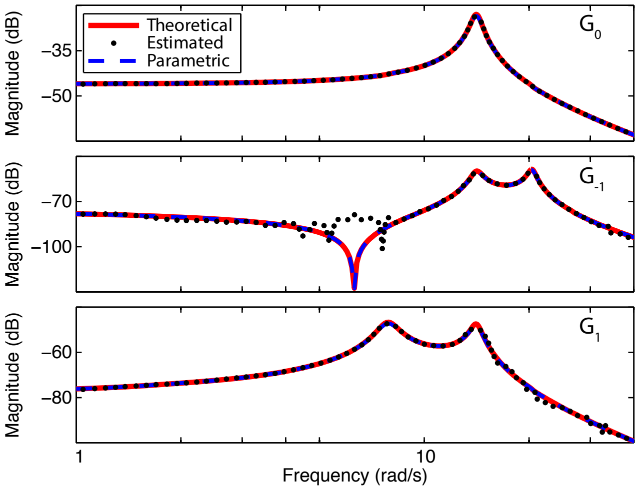

Fig. 2. Magnitudes of HTF components for theoretically computed (solid red), estimated (dotted black) and parametrically fitted (dashed blue) models.

of measurement delays on system response. This yields input–output data we use to estimate harmonic transfer functions as described in Section 2.2. At this stage, as noted before, the identification process will be unaware of the amount of input and measurement delays that are present in the system.

4.4 Parametric Identification with Harmonic Transfer Functions

Fig. 2 illustrates the magnitudes of harmonic transfer functions obtained through the theoretical derivations of Section 4.2 (solid red) and the data-driven estimates of Section 4.3 (dotted black). However, the theoretical transfer functions rely on the knowledge of dynamic systems parameters which may normally not be available for a physical system. Consequently, before we proceed with the estimation of delays using the phase characteristics, we first estimate these unknown parameters k and c in (13) using the identification strategy presented in Uyanik et al. (2015a). Equation (8) shows that the input and measurement delay does not effect the magnitude of the harmonic transfer functions. We can hence use data from all nine experiments with different delays, resulting in estimated values $\hat{k} = 200$ and $\hat{c} = 2.12$ for the spring and damping constants, respectively. This yields parametric magnitude responses shown in Fig. 2 in dashed blue, closely matching the theoretical derivations with the exact parameter values. Phase responses for this parametric model will be used in the next section to identify input and measurement delays in the system.

4.5 Estimation of Input and Measurement Delays

As is evident from (9), a comparison of phase responses associated with HTF components for the models with and without time delay can be used to separately estimate input and measurement delays. These phase plots are illustrated in Fig. 3, with the undelayed parametric model and the delayed input–output estimates are shown in solid blue and dotted black, respectively. The phase error

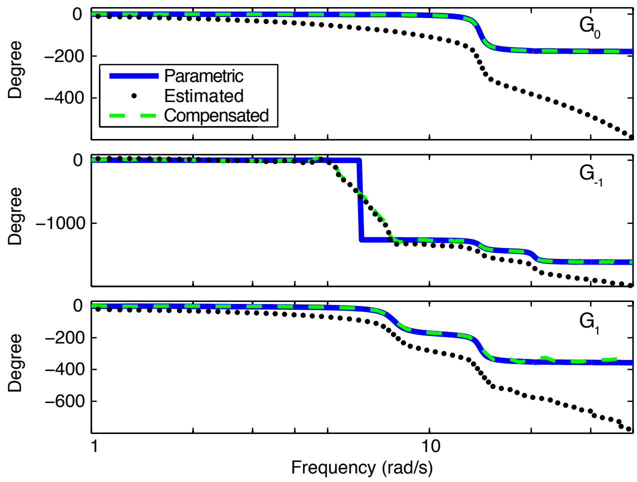

Fig. 3. Phase responses of HTF components for the parametrically fitted (dashed blue) and estimated (dotted black) models. The dashed green plot shows the phase responses of the estimated model compensated with the identified input and measurement delays.

between these two responses can be expressed using (9) with respect to input and measurement delays as

$$\underline{/G_{err}} = \underline{/G_m(j\omega)} - \underline{/\hat{G}_m(j\omega)} + [(\omega - m\omega_p)\tau_u + \omega\tau_y]. \quad (15)$$

Based on this expression, we formulate a minimization problem as a function of unknown input and measurement delays, taking the form

$$(\tau_u^*, \tau_y^*) = \underset{(\tau_u, \tau_y)}{\arg\min} \sqrt{\int_0^{40} (|\hat{G}_m(j\omega)|\, \underline{/G_{err}})^2\, d\omega} \; . \quad (16)$$

Green dashed plots in Fig. 3 show phase responses of the identified system compensated with the delay estimates resulting from this minimization problem.

More systematically, Table 1 shows estimation results for input and measurement delays by only using phase responses from $\hat{G}_0$, $\hat{G}_{-1}$ and $\hat{G}_1$ with respect to parametrically identified harmonic transfer functions. As predicted by (9), $\hat{G}_0$ alone can not separate the effects of input and measurement delays. Consequently, we evaluate the estimation performance of the total delay in the system for this case. Table 1 shows that individual estimates of both types of delay stay below 5% for all nine experiments with differing amounts of actual delays.

5. CONCLUSION

In this paper, we presented a system identification strategy to estimate input and measurement delays for a hybrid, vertical, spring–mass–damper system. We first show how rhythmic locomotor systems can be identified in frequency domain using data-driven system identification techniques. To this end, we linearize the system dynamics around an asymptotically stable limit cycle and approximate the hybrid transitions between different states as a time-periodic behavior, so that we obtain a linear time periodic system representation for our simple hybrid model.

Our system identification process requires perturbing the limit cycle with chirp signals and recording deviations from the limit cycle as measured in the system output.

However, our goal is to perform system identification under input and measurement delay and estimate the delay in the system using our transfer function estimates. To accomplish this, we performed nine experiments with different input and measurement delays in the system and estimated harmonic transfer functions corresponding to input–output characteristics of the system.

As for LTI transfer functions, we show that input and measurements delay on harmonic transfer functions do not effect the magnitudes of harmonic transfer functions. Therefore, we perform parametric identification based on the estimated harmonic transfer functions by only using the magnitude responses. The key point in our theoretical analysis is that the use of harmonic transfer functions allows us to independently estimate input and measurement delay in the system when the higher order harmonics are considered in the estimation process. We compare the phase response of the estimated and parametrically identified harmonic transfer functions for this purpose and estimate input and measurement delay in the system for the nine different experiment performed in this study.

REFERENCES

Altendorfer, R., Koditschek, D.E., and Holmes, P. (2004). Stability analysis of a clock-driven rigid-body SLIP model for RHex. *Int J Robot Res*, 23(10-11), 1001–1012.

Anderson, R. and Spong, M.W. (1989). Bilateral control of teleoperators with time delay. *IEEE Trans Autom Control*, 34(5), 494–501.

Ankarali, M.M. and Saranli, U. (2010). Stride-to-stride energy regulation for robust self-stability of a torque-actuated dissipative spring-mass hopper. *Chaos*, 20(3), 033121.

Ankarali, M.M. and Cowan, N.J. (2014). System identification of rhythmic hybrid dynamical systems via discrete time harmonic transfer functions. In *Proc IEEE Int Conf on Decision and Control*. Los Angeles, CA, USA.

Cowan, N.J., Ankarali, M.M., Dyhr, J.P., Madhav, M.S., Roth, E., Sefati, S., Sponberg, S., Stamper, S.A., Fortune, E.S., and Daniel, T.L. (2014). Feedback control as a framework for understanding tradeoffs in biology. *Integr Comp Biol*, 54(2), 223–237. doi:10.1093/icb/icu050.

Cowan, N.J., Lee, J., and Full, R.J. (2006). Task-level control of rapid wall following in the American cockroach. *J Exp Biol*, 209(9), 1617–1629. doi:10.1242/jeb.02166.

Elzinga, M.J., Dickson, W.B., and Dickinson, M.H. (2012). The influence of sensory delay on the yaw dynamics of a flapping insect. *J R Soc Interface*, 9(72), 1685–1696.

Full, R.J. and Tu, M.S. (1991). Mechanics of a rapid running insect: two-, four-, and six-legged locomotion. *J Exp Biol*, 156, 215–231.

Galloway, K.C., Haynes, G.C., Ilhan, B.D., Johnson, A.M., Knopf, R., Lynch, G., Plotnick, B., White, M., and Koditschek, D.E. (2010). X-rhex: A highly mobile hexapedal robot for sensorimotor tasks. Technical report, University of Pennsylvania.

Grizzle, J., Abba, G., and Plestan, F. (2001). Asymptotically stable walking for biped robots: analysis via systems with impulse effects. *IEEE Trans Autom Control*, 46(1), 51–64.

Holmes, P.J., Full, R.J., Koditschek, D.E., and Guckenheimer, J. (2006). The dynamics of legged locomotion: Models, analyses, and challenges. *SIAM Rev*, 48(2), 207–304.

Kataria, A., Özbay, H., and Hemami, H. (2002). Controller design for natural and robotic systems with transmission delays. *J Robotic Syst*, 19(5), 231–244.

Kiemel, T., Logan, D., Ivanenko, Y., Lacquaniti, F., and Jeka, J.J. (2013). Characterizing perturbations of human walking in the frequency domain. In *Dynamic Walking*. Pittsburgh, PA, USA.

LaBarbera, M. (1983). Why the wheels won't go. *Amer Nat*, 121(3), 395–408.

Miller III, W.T. (1989). Real-time application of neural networks for sensor-based control of robots with vision. *IEEE Trans Syst, Man, Cybern*, 19(4), 825–831.

Raibert, M.H. (1986). *Legged Robots That Balance*. MIT Press, Cambridge, MA, USA.

Saranli, U., Arslan, O., Ankaralı, M.M., and Morgül, Ö. (2010). Approximate analytic solutions to non-symmetric stance trajectories of the passive spring-loaded inverted pendulum with damping. *Nonlinear Dynam*, 62, 729–742.

Saranli, U., Buehler, M., and Koditschek, D.E. (2001). RHex: A simple and highly mobile robot. *Int J Robot Res*, 20(7), 616–631.

Seipel, J. and Holmes, P. (2007). A simple model for clock-actuated legged locomotion. *Regul Chaotic Dyn*, 12, 502–520.

Siddiqi, A. (2001). *Identification of the Harmonic Transfer Functions of a Helicopter Rotor*. M.Sc., Massachusetts Institute of Technology, Dept. of Aeronautics and Astronautics.

Sponberg, S. and Full, R.J. (2008). Neuromechanical response of musculo-skeletal structures in cockroaches during rapid running on rough terrain. *J Exp Biol*, 211(3), 433–446.

Tian, Y.P. and Liu, C.L. (2008). Consensus of multi-agent systems with diverse input and communication delays. *IEEE Trans Autom Control*, 53(9), 2122–2128.

Uyanik, I., Ankarali, M.M., Cowan, N.J., Morgül, Ö., and Saranli, U. (2015a). System identification of a hybrid vertical spring mass damper via harmonic transfer functions as a step towards data-driven models for legged locomotion. In *Int Conf on Advanced Robotics*. To Appear.

Uyanik, I., Ankarali, M.M., Cowan, N.J., Saranli, U., and Morgül, Ö. (2015b). Identification of a vertical hopping robot model via harmonic transfer functions. *T I Meas Control*. To Appear.

Uyanik, I., Morgül, Ö., and Saranli, U. (2015c). Experimental validation of a feed-forward predictor for the spring-loaded inverted pendulum template. *IEEE Trans Robot*, 31(1), 208–216.

Wereley, N.W. (1991). *Analysis and Control of Linear Periodically Time Varying Systems*. Ph.d., Massachusetts Institute of Technology, Dept. of Aeronautics and Astronautics.

Westervelt, E.R., Grizzle, J.W., Chevallereau, C., Choi, J.H., and Morris, B. (2007). *Feedback control of dynamic bipedal robot locomotion*, volume 28. CRC press.

Wooden, D., Malchano, M., Blankespoor, K., Howardy, A., Rizzi, A., and Raibert, M. (2010). Autonomous navigation for bigdog. In *Proc IEEE Int Conf Robot Autom*, 4736–4741.